INTERNATIONAL JOURNAL OF HEAT AND TECHNOLOGY

ISSN: 0392-8764
Vol. 35, No. 3, September 2017, pp. 619-625
DOI: 10.18280/ijht.350319

A publication of IIETA
International Information and Engineering Technology Association
Advancing the World of Information and Engineering
http://www.iieta.org/Journals/IJHT

Numerical study of nanofluid heat transfer SiO_2 through a solar flat plate collector

Ammar Maouassi[1, 2*], Abdelhadi Baghidja[1, 2], Said Daoud[3], Noureddine Zeraibi[3]

[1] Department of Mechanical Engineering, University of Constantine1, Constantine 25000, Algeria
[2] Renewable Energy and Sustainable Development Laboratory (LERDD), University of Constantine1, Constantine 25000, Algeria
[3] Department of Transportation of Hydrocarbons, University of Boumerdès, Boumerdès 35000, Algeria

Email: maouassi.ammar@umc.edu.dz

ABSTRACT

This paper illustrates how practical application of nanoparticles (SiO_2) as working fluid to stimulate solar flat plate collector efficiency with heat transfer modification properties. A numerical study of nanofluids laminar forced convection, permanent and stationary (SiO_2), is conducted in a solar flat plate collector. The effectiveness of these nanofluids are compared to conventional working fluid (water), wherein the dynamic and thermal properties are evaluated for four volume concentrations of nanoparticles (1%, 3%, 5% and 10%), and this done for Reynolds number from 25 to 900. Results from the application of those nonfluids are obtained versus average temperature; pressure drop coefficient and Nusselt number are discussed later in this paper. Finally, we concluded that heat transfer increases with increasing both nanoparticles concentration and Reynolds number.

Keywords: Solar Energy, CFD, Nanofluid, Heat Transfer, Sio_2 Nanoparticles, Solar Flat Plate Collector.

1. INTRODUCTION

Thermal solar energy has a major importance in the world because it's clean, renewable and sustainable, it has several practical and industrial applications, including electrical production, energy systems heating and cooling; in which the principal elements in these systems are the solar collectors which convert solar radiation to thermal energy then transfer it towards the carrying fluid [1]. The most known solar collectors used are the flat-plat collector. However, this type has relatively low energy efficiency and low outlet temperatures. Recently, several studies have been carried out on the flat plate solar collector to overcome these disadvantages [2, 3], in addition to these classical studies or methods, which are used to increase the thermal efficiency of this kind of solar collector, one of the latest effective method is to replace the conventional working fluid by other fluids, which having higher thermal properties.

The idea to improve thermo-physical properties of conventional fluids is adding solid particles with a high thermal characteristics and nano-size, inside basic fluid. This new generation of fluids named Nanofluids; this term was introduced first by Choi [4], and usually stills use to characterize this colloidal suspension type. After these initiative studies of the ARGONNE laboratory group, several studies have been carried out in this research area to understand the thermohydraulic behavior of this new heat transfer fluid generation [5-12]. Nanoparticles suspension within the conventional heat transfer fluid increases its thermal conductivity and consequently improves the heat transfer [5]. Free convection heat transfer in a porous medium with nanofluid was examined by Sheikholeslami et al. [6, 7] they found that the improvement of the heat transfer coefficient is related to the increase of nanoparticles volume concentration.

In the same research field context, Sheikholeslami [8] carried out a 3D numerical study on forced convection heat transfer, it is found that the temperature gradient on the hot surface side increases with the increase of the nanoparticles volume fraction and both Reynolds and Darcy numbers. The magnetic field Influence on nanofluids hydrothermal behavior, Sheikholeslami used two different nanofluid types, Fe_3O_4-H_2O nanofluid [9, 11] and CuO-H_2O nanofluid [5, 6, 12]. These studies demonstrate when Nusselt number increases, it has a direct relation with Rayleigh number and nanoparticles volume concentration; whereas inverse relation with Hartmann number when decreasing. Despite the fact that there is no commercial solar collector available that uses these nanofluids, there are experimental studies that confirm its effectiveness by adding nanoparticle to improve the

thermal efficiency, Natarajan et al. [13] found that if the nanofluids are used as working fluids, the energy efficiency of solar water heaters increases significantly compared to conventional fluids. On the other hand, the dispersion of the nanoparticles gives an important increase in the heat transfer coefficient [14-19]. Hence, they found that it is possible to reduce the exchange surface and improve the efficiency of these devices, which confirms the results of [13]. Nasrin et al. [20] carried out a numerical study of forced convection heat transfer through a flat plate solar collector, the geometry is tested for 2D case, then 3D, where water and Cu-H_2O nanofluid are used as a working fluid, the results obtained show that 3D simulation is more efficient than 2D, and the increase of nanoparticles volume concentration gives an improvement in heat transfer rate reach 17% and about 8% for thermal efficiency of solar collector.

In this paper, we present the study of heat transfer of nanofluid (SiO_2) flows through a solar flat plate collector. In the first part, we describe the problem and present the boundary conditions. After grid independence study, then we validated the results by comparing them with previous literature reports.

The key part of this work is to involve the simulation with the interpretation of numerical results obtained for this case, where the effect of nanoparticles is shown for various volume concentration and Renolds number, and studied systematically. At the end, this paper is footed by conclusion which summarizes the main results obtained.

2. MATHEMATICAL FORMULATION

The flow domain consists of an absorber plate and circular absorber tube. The absorber plate is covered with glass plate with an air gap. Design parameters and fixed geometric parameters have been taken similar to Karanth et al. [21], as indicated in Table 1.

The forced heat transfer of nanofluide under laminar flow inside the absorbent tube, as shown in Fig. 1, the flow is assumed steady and the fluid possesses uniform axial velocity V_0 and temperature T_0 profiles at the inlet of tube.

2.1 Assumptions

The nanoparticles used in practical applications of heat exchange are very thins (≤ 50 nm), then the liquid-particle mixture may easily be fluidized and considered as a homogenous single-phase fluid [22].

By assuming negligible thermal equilibrium and slip between the phases, the apparent thermal properties of nanofluids can be estimated by using classical relationships of two-component mixture [23], and the mixture considered as a conventional single-phase fluid [22].

Table 1. Design parameters of solar collector

	absorber plate (mm)	Tube (mm)	glass plate (mm)	air gap (mm)
length	1000	1010	1000	1000
wide	150	-	150	150
diameter	-	10	-	-
thickness	2	1	2	3

2.2 Governing equations and boundary condition

Under the previous assumptions, the general governing equations are:

2.2.1 Continuity equation

$$\frac{\partial}{\partial x_j}\left(\rho_{nf}\, u_j\right) = 0 \tag{1}$$

2.2.2 Momentum equation

$$\rho_{nf}\,\frac{\partial\left(u_i u_j\right)}{\partial x_j} = -\frac{\partial P}{\partial x_i} + \frac{\partial}{\partial x_j}\left(\mu_{nf}\,\frac{\partial u_i}{\partial x_j}\right) \tag{2}$$

2.2.3 Energy equation

$$\frac{\partial}{\partial x_j}\left(u_j\, T\right) = \frac{k_{nf}}{\rho_{nf}\, Cp_{nf}}\left(\frac{\partial^2 T}{\partial x_j^2}\right) \tag{3}$$

The physical properties of nanofluid, nanofluid density $\boldsymbol{\rho_{nf}}$ [24], viscosity $\boldsymbol{\mu_{nf}}$ [25], Thermal conductivity $\boldsymbol{k_{nf}}$ [26] and Nanofluid specific heat $\boldsymbol{Cp_{nf}}$ [22] are given with the below equations:

$$\rho_{nf} = \rho_s\,\varphi + \rho_f\left(1-\varphi\right) \tag{4}$$

$$\mu_{nf} = \left(1+2.5\varphi\right)\mu_f \tag{5}$$

$$k_{nf} = \frac{k_s - 2k_f - 2\varphi\left(k_f - k_s\right)}{k_s + 2k_f + \varphi\left(k_f - k_s\right)}\,k_f \tag{6}$$

$$Cp_{nf} = \frac{\rho_s Cp_s\,\varphi + \rho_f Cp_f\left(1-\varphi\right)}{\rho_{nf}} \tag{7}$$

For boundary conditions and operating parameters are taken similar to Karanth et al. [21]. For inlet, a 'velocity inlet' boundary condition is specified and an 'outflow' condition is specified at the outlet for the water domain. The glass material is made up of Borosilicate, which has a refractive index of 1.47. Absorber plate and absorber tube are made up of copper material. Wall boundary conditions used to bound fluid and solid regions. The interface between water and absorber tube is defined as coupled wall condition. In the top of collector, a constant solar heat flux equal to 800W/m^2 are imposed.

Table 2. Properties of various used material

Properties	Absorber P&T	Glass Plate	Air
ρ (kg/m^3)	8978	2230	1.225
Cp (J/kg°k)	381	750	1006.4
K (W/m°k)	387.6	1.14	0.0242

2.3 Skin friction coefficient

The skin friction coefficient for the fully developed laminar flow in a circular tube is given by

$$\lambda = \tau_s \frac{\rho u_m^2}{2} \tag{8}$$

where τ_s is local shear stress, and u_m is the mean velocity given by

$$u_m = \frac{\int_0^R \rho\, u\, 2\pi r dr}{\int_0^R \rho\, 2\pi r dr} = \frac{2}{R^2}\int_0^R u\, r dr \tag{9}$$

2.4 Local Nusselt number

The Nusselt number, which represents the dimensionless temperature gradient at the surface (Eq. 14) and provides a measure of the convection coefficient, is defined as

$$Nu_{x,nf} = \frac{h_{nf,x} D}{k_f} \tag{10}$$

The local heat flux at the surface is obtained by applying Fourier's law to the fluid at r = R

$$q''_{sf} = -k_{nf}\left(\left.\frac{\partial T}{\partial r}\right|_{r=R}\right)_{sf} \tag{11}$$

Near the wall of tube absorber, the surface heat flux is equal to the convective flux the fluid (no-slip condition), which is expressed by Newton's law of cooling

$$q''_{sf} = q''_{conv} = h_{nf,x}\left(T_{w,x} - T_{m,x}\right) \tag{12}$$

where $T_{w,x}$, $T_{m,x}$ are the local wall temperature and mean fluid temperature respectively, the mean temperature of a fluid flowing in a circular pipe of radius R is given by

$$T_m = \frac{\int_0^R \rho c_p\, u T\, 2\pi r dr}{\int_0^R \rho c_p\, u\, 2\pi r dr} = \frac{2}{u_m R^2}\int_0^R T\, u\, r dr \tag{13}$$

By combining the foregoing equations (Eqs. 11 and 12), we obtain the local convection coefficient

$$h_{nf,x} = -\frac{k_{nf}}{T_{w,x} - T_{m,x}}\left(\left.\frac{\partial T}{\partial r}\right|_{r=R}\right)_{nf} \tag{14}$$

And the Nusselt number of nanofluid are given by

$$Nu_{x,nf} = -\frac{2k_{nf}}{k_f}\frac{R}{T_{w,x} - T_{m,x}}\left(\left.\frac{\partial T}{\partial r}\right|_{r=R}\right)_{nf} \tag{15}$$

The rate of the improvement in the heat transfer coefficient is calculated as follows

$$Nu\,(\%) = \frac{Nu_{nf} - Nu_{water}}{Nu_{water}} \times 100 \tag{16}$$

3. NUMERICAL METHOD AND CODE VALIDATION

To conduct numerical simulation, the computational domain was meshed with control volumes built around each grid using GAMBIT (version 2.4.6), which is the pre-processor for FLUENT (version 6.3). Numerical simulation was carried out using steady state implicit pressure based solver, which is an in-built in the commercially available software FLUENT (version 6.3). Governing partial differential equations, for mass and momentum, are solved for the steady incompressible flow. The velocity-pressure coupling is affected through SIMPLE algorithm developed by Patankar [27]. Second order upwind schemes were chosen for the solution schemes laminar flow condition was used.

3.1 Meshing

The computational domain was meshed and done by using appropriate grid cells, with suitable size. Three dimensional computational domains are built and used, as shown in Fig. 1. To solve the previous system of governing equations (1-3), the computational domain was meshed with the finite control volume method [28] which has been successfully used by several authors [29, 30]. To compute the combined convection-and-diffusion fluxes of heat the upwind method are used, where the upwind scheme of the second order has been used throughout for computing heat and momentum fluxes.

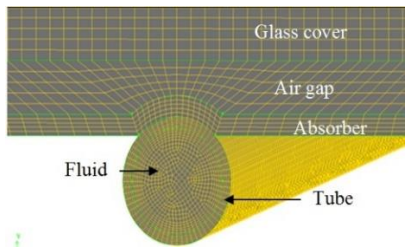

Figure 1. Mesh of the computational domain

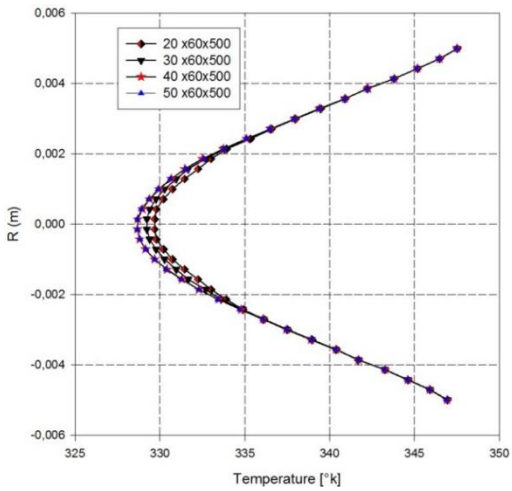

Figure 2. Mesh validation curves for the outlet temperature evolution

Several non-uniform grids have been thoroughly tested to ensure the accuracy and the consistency of numerical results, which has shown that the 40 x 60x 500 non-uniform grid (32, 24 and 155 nodes, respectively, along the radial, tangential and axial directions) appears satisfactory for the absorber

tube (fig. 2); with refining mesh near the tube wall and the entrance region.

3.2 Code validation

Figure 3 represent the temperature distribution on the absorber plate for different values of inlet velocity (V= 0.001, V= 0.005, V= 0.01 and V= 0.05 m/s). The axial temperatures evolution of the working fluid along the absorber tube are represented in Fig. 4; with different axial flow velocities V_Z ranging from 0.0001 to 0.05 m/s, in the same boundary conditions used by Karanth et al. [21].

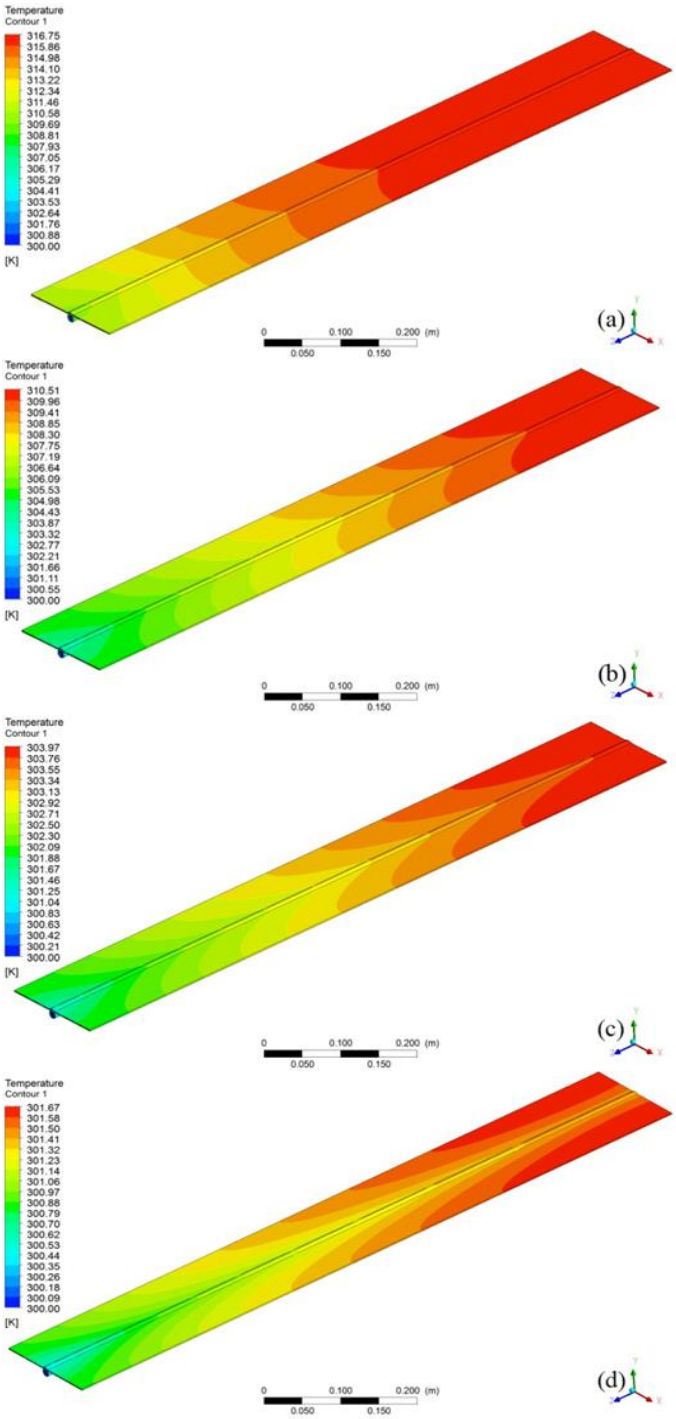

Figure 3. Temperature distribution on the absorber for (a) V= 0.001m/s, (b) V=0.005m/s, (c) V=0.01m/s, (b) V=0.05m/s

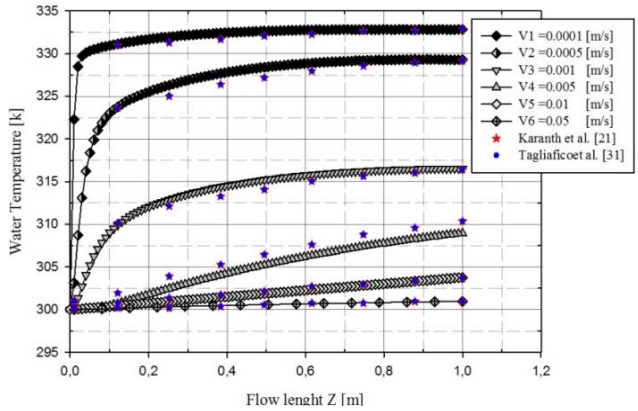

Figure 4. Validation of temperature contour of absorber plate Comparison of fluid temperature distribution between this study and these of Karanth et al. [21] & Tagliafico et al. [31]

The numerical results obtained by Karanth et al. [21], provide an excellent test tool to validate our calculation code; by comparing the obtained numerical results with those published by Karanth et al. [21] and Tagliafico et al. [31] literatures, we notice a very good matching between our results and those of the authors; hence our simulation is successfully validated.

4. RESULTS AND DISCUSSION

We study the nanofluids heat transfer flow inside an absorbent tube, where he heated by the absorbent plaque. We consider the flow regime as laminar, and varying the number of Reynolds between 25 and 900, for the different nanoparticles concentrations (1%, 3%, 5%, and 10%). Then we plot the results, pressure drop coefficient and Nusselt number.

4.1 Pressure drop coefficient

Figures 5.a and 5.b, represent the variation of skin friction coefficient versus volume concentration "ϕ" and Reynolds number "Re". We note a slight increase in skin friction coefficient (λ) when the Reynolds number is low (Re ≤ 100) as showing in Fig. 5.a, this slight increase in λ is due to the presence of the nanoparticles and lower fluid flow velocities, but when the Reynolds number exceeds 100 this problem doesn't occur.

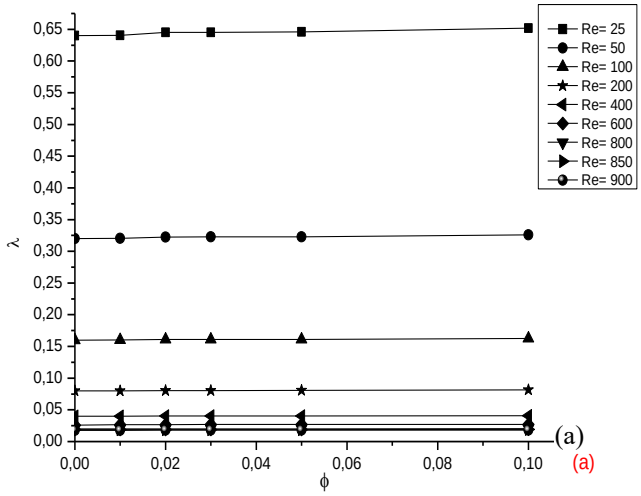

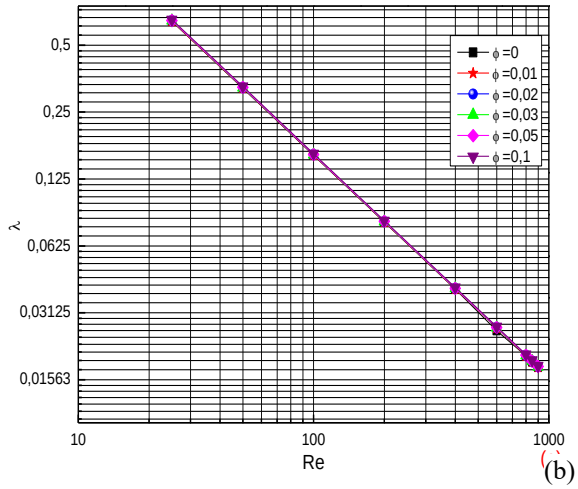

Figure 5. Skin friction coefficient versus: (a) volume fraction of SiO_2 nanoparticles and (b) Reynolds numbers

Fig. 5.b, it will be noted that for the same Reynolds number, and despite the variation in the nanoparticles concentration volume; the λ value is almost identical, this confirm and supports the previous result in Fig. 5.a. These results, therefore, reflect the insignificant influence of the nanoparticles volume concentration on the skin friction coefficient λ.

4.2 Nusselt number

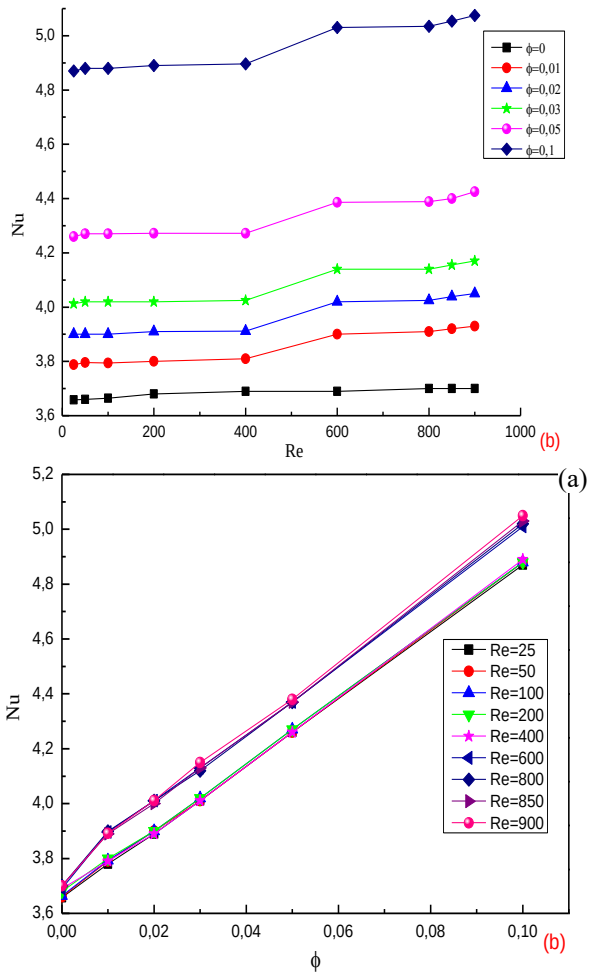

Figure 6. Heat transfer coefficient versus: (a) Reynolds number and (b) different concentrations of SiO_2 nanoparticles

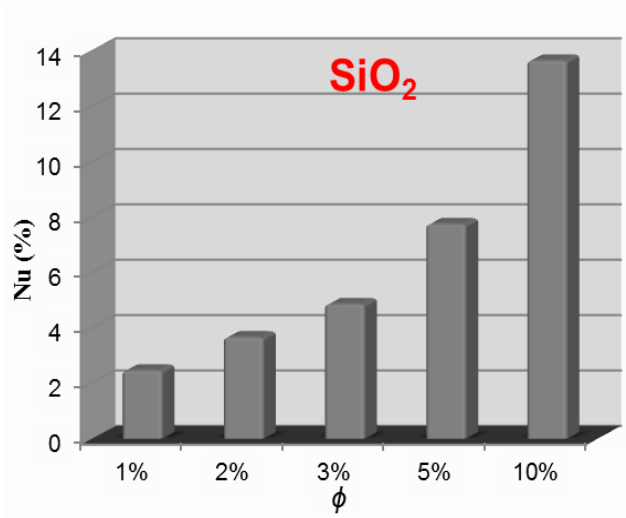

Figure 7. The improvement rate of heat transfer coefficient

Figures 6.a and 6.b, represents the Nusselt number "Nu" evolution as a function of Reynolds number and the volume fraction "ϕ".

We note, a significant increase of Nusselt number with the increase in nanoparticle volume concentration for all its value as showing in figure 6.a, so in relation with pure water, whereas, a slight increase versus Reynolds number as showing in figure 6.b. Each increase in the volume concentration is accompanied with a significant increase in the Nusselt number, consequently the heat transfer intense through the working fluid.

In the Figure 7, represent the comparison in term of rate improvement of heat transfer coefficient for various volume concentrations of nanoparticles.

We notice then, a considerable increase of the improvement rate compared to pure water which can reach an average value of 13.7 % for ϕ= 10 %.

5. CONCLUSIONS

In this paper, the flow and heat transfer characteristics of SiO_2-water nanofluid for arrange of the Reynolds number (25to 900) with a wide range of volume concentration (0 to 10%) are studied numerically.

We can confirm from analyze of thermal-hydraulic properties of nanofluids, on one hand, the presence of nanoparticles in the base fluid (pure water) increases significantly Nusselt number, that is also growing with the increase of volume fraction, the increase in heat coefficient results improve the heat transfer through the energy systems compared to the base fluid (pure water) case. On the other hand, the gain in heat is accompanied by a slight increase in skin friction coefficient for the low Reynolds numbers due to the presence of the nanoparticles and lower flow velocities, but when the Reynolds number exceeds 100 this problem doesn't occur.

The results show that, Nusselt number and heat transfer coefficient, of nanofluid are strongly dependent on nanoparticle and increase by increasing of the volume concentration of nanoparticles, and the insignificant influence of the nanoparticles volume concentration on the skin friction coefficient.

REFERENCES

[1] Rovense F., Amelio M., Ferraro V., Scornaienchi N.M. (2016). Analysis of a concentrating solar power tower operating with a closed joule Brayton cycle and thermal storage, *International Journal of Heat and Technology*, Vol. 34, No. 3, pp. 485-490. DOI: 10.18280/IJHT.340319

[2] Nasrin R., Alim M.A. (2015). Thermal performance of nanofluid filled solar flat plate collector, *International Journal of Heat and Technology*, Vol. 33, No. 2, pp. 17-24. DOI: 10.18280/IJHT.330203

[3] Zhuang C., Fu B., Huang G., Zhang H. (2016). Optimization of the structure of a solar air heater fitted with V-shaped perforated baffles, *International Journal of Heat and Technology*, Vol. 34, No. 4, pp. 604-610. DOI: 10.18280/IJHT.340408

[4] Choi S.U.S., Eastman J.A. (1995). Enhancing thermal conductivity of fluids with nanoparticles, *ASME Int Mech Eng Congr Expo*, San Francisco, USA, Vol. 66, pp. 99-105.

[5] Sheikholeslami M. (2014). Effect of uniform suction on nanofluid flow and heat transfer over a cylinder, *J Braz. Soc. Mech. Sci. Eng*, Vol. 37, pp. 1623-1633. DOI: 10.1007/S40430-014-0242-Z

[6] Sheikholeslami M. (2017). Influence of magnetic field on nanofluid free convection in an open porous cavity by means of lattice Boltzmann Method, *Journal of Molecular Liquids*, Vol. 234, pp. 364-374. DOI: 10.1016/J.MOLLIQ.2017.03.104

[7] Sheikholeslami M. (2017). CuO-water nanofluid free convection in a porous cavity considering Darcy law, *Eur. Phys. J. Plus*, Vol. 132, pp. 1-11. DOI: 10.1140/EPJP/I2017-11330-3

[8] Sheikholeslami M. (2017). Magnetohydrodynamic nanofluid forced convection in a porous lid driven cubic cavity using Lattice Boltzmann Method, *Journal of Molecular Liquids*, Vol. 231, pp. 555-565. DOI: 10.1016/J.MOLLIQ.2017.02.020

[9] Kandelousi M.S. (2014). Effect of spatially variable magnetic field on ferrofluid flow and heat transfer considering constant heat flux boundary condition, *Eur. Phys. J. Plus*, Vol. 129, pp. 1-12. DOI: 10.1140/EPJP/I2014-14248-2

[10] Sheikholeslami M. (2017). Magnetic field influence on nanofluid thermal radiation in a cavity with tilted elliptic inner cylinder, *Journal of Molecular Liquids*, Vol. 229, pp. 137-147. DOI: 10.1016/J.MOLLIQ.2016.12.024

[11] Sheikholeslami M. (2017). Numerical simulation of magnetic nanofluid natural convection in porous media, *Physics Letters A*, Vol. 381, pp. 494-503. DOI: 10.1016/J.PHYSLETA.2016.11.042

[12] Sheikholeslami M. (2017). Influence of Lorentz forces on nanofluid flow in a porous cylinder considering Darcy model, *Journal of Molecular Liquids*, Vol. 225, pp. 903-912. DOI: 10.1016/J.MOLLIQ.2016.11.022

[13] Natarajan E., Sathish R. (2009). Role of nanofluids in solar water heater, *Int J. Adv Manuf Technol*, Vol. 45, pp. 1-5. DOI: 10.1007/S00170-008-1876-8

[14] Sokhansefat T., Kasaeian A.B., Kowsary F. (2014). Heat transfer enhancement in parabolic trough collector tube using Al_2O_3/synthetic oil nanofluid, *J. Renewable and Sustainable Energy Reviews*, Vol. 33, pp. 636-644. DOI: 10.1016/J.RSER.2014.02.028

[15] Otanicar T.P., Phelan P.E., Prasher R.S., Rosengarten G., Taylor R.A. (2010). Nanofluid-based direct absorption solar collector, *J. Renewable and Sustainable Energy*, Vol. 2, p. 13. DOI: 10.1063/1.3429737

[16] Faizal M., Saidur R., Mekhilef S., Alim M.A. (2013). Energy, economic and environmental analysis of metal oxides nanofluid for flat-plate solar collector, *J. Energy Conversion and Management*, Vol. 76, pp. 162-168. DOI: 10.1016/J.ENCONMAN.2013.07.038

[17] Said Z., Sajid M.H., Alim M.A., Saidur R., Rahim N.A. (2013). Experimental investigation of the thermophysical properties of AL_2O_3-nanofluid and its effect on a flat plate solar collector, *Int Commu in Heat and Mass Transfer*, Vol. 48, pp. 99-107. DOI: 10.1016/J.ICHEATMASSTRANSFER.2013.09.005

[18] He Q., Zeng S., Wang S. (2015). Experimental investigation on the efficiency of flat-plate solar collectors with nanofluids, *J. Applied Thermal Engineering*, Vol. 88, pp. 165-171. DOI: 10.1016/J.APPLTHERMALENG.2014.09.053

[19] Menbari A., Alemrajabi A.A., Rezaei A. (2016). Heat transfer analysis and the effect of CuO/Water nanofluid on direct absorption concentrating solar collector, *J. Applied Thermal Engineering*, Vol. 104, pp. 176-183. DOI: 10.1016/J.APPLTHERMALENG.2016.05.064

[20] Nasrin R., Alim M.A., Ahmed S.R. (2016). Comparative study between 2D and 3D modeling of nanofluid filled flat plate solar collector, *International Journal of Heat and Technology*, Vol. 34, No. 3, pp. 604-610. DOI: 10.18280/IJHT.340326

[21] Karanth K., Manjunath M., Sharma N. (2011). Numerical simulation of a solar flat plate collector using discrete transfer radiation model (DTRM) – a CFD approach, *In: Proceedings of the world congress on engineering*, London, pp. 2355-2360.

[22] Xuan Y., Roetzel W. (2000). Conception for heat transfer correlation of nanofluids, *Int J. Heat and Mass Transfer*, Vol. 43, pp. 3701-3707. DOI: 10.1016/S0017-9310(99)00369-5

[23] Pak B.C., Cho Y.I. (1998). Hydrodynamic and heat transfer study of dispersed fluids with submicron metallic oxide particles, *J. Experimental Heat Transfer*, Vol. 11, pp. 151-170. DOI: 10.1080/08916159808946559

[24] Zhang X., Gu H., Fujii M. (2007). Effective thermal conductivity and thermal diffusivity of nanofluids containing spherical and cylindrical nanoparticles, *J. Experimental Thermal and Fluid Science*, Vol. 31, pp. 593-599. DOI: 10.1016/j.expthermflusci.2006.06.009

[25] Brinkman H.C. (1952). The viscosity of concentrated suspensions and solution, *J. Chemistry Physics*, Vol. 20, pp. 571-581. DOI: 10.1063/1.1700493

[26] Maxwell J.C. (1892). *A Treatise on Electricity and Magnetism*, 3rd ed., Vol. 2, Clarendon Press, Oxford, 1904, pp. 430-441.

[27] Patankar V.S. (1980). *Numerical Heat Transfer and Fluid Flow*, 1st ed., Hemisphere Publishing Corporation, New York, pp. 113-125.

[28] Versteeg H., Malalasekera W. (1996). *An Introduction to Computational Fluid Dynamics: The Finite Volume Method*, 2nd ed., Longman Group Lt, England, pp. 85-

133.
[29] Beyers J.H.M., Harms T.M., Kröger D.G. (2001). A finite volume analysis of turbulent convective heat transfer for accelerating radial flows, *J. Numerical Heat Transfer*, Vol. 40, pp. 117-138. DOI: 10.1080/104077801750468453
[30] Maïga S.E.B., Nguyen C.T., Galanis N., Roy G. (2004). Heat transfer behaviors of nanofluids in uniformly heated tube, *Superlatives and Microstructures*, Vol. 35, pp. 543-557. DOI: 10.1016/J.SPMI.2003.09.012
[31] Tagliafico I.A., Scarpa F., Rosa M.D. (2014). Dynamic thermal models and CFD analysis for flat-plate thermal solar collectors – a review, *Renew and Sust Energy Rev*, Vol. 2, No. 30, pp. 526-537. DOI: 10.1016/J.RSER.2013.10.023

NOMENCLATURE

Latins Symbols

Cp	Specific heat
h	Heat transfer coefficient
k	Thermal conductivity
T	Temperature
L	Length of the absorber tube
D	Diameter of the absorber tube
Nu	Nusselt number
Re	Reynolds number
u	axial velocity
R	tube radius
q″	heat flux

Greek symbols

ϕ	Volume concentration
λ	skin friction coefficient
μ	Viscosity
ρ	Density

Subscripts

s	Solid
f	Fluid
nf	Nanofluid
m	mean value
w	wall
sf	surface